Suplemento de la Revista Mexicana de Física **3** 020711 (2022) 1–6

ν-e Scattering radiative corrections in a short baseline experiment

O. G. Miranda and G. Moreno-Granados

Departamento de Física, Centro de Investigación y de Estudios Avanzados del IPN, Apartado Postal 14-740 07000 Mexico, Distrito Federal, Mexico.
e-mail: omr@fis.cinvestav.mx; gmoreno@fis.cinvestav.mx

C. A. Moura

Universidade Federal do ABC (UFABC), Santo André - SP, 09210-580, Brazil.
e-mail: celio.moura@ufabc.edu.br

Received 30 December 2021; accepted 7 February2022

Precision tests in future long-baseline experiments will measure neutrino oscillation properties with high accuracy. Besides, with their near detectors will be possible to perform measurements with high statistics, such as neutrino scattering with electrons, among other neutrino interactions. Near detectors will give the chance to measure the radiative corrections of this process with unprecedented precision. This work will discuss how the test of the radiative corrections in the neutrino-electron scattering may measure the neutrino charge radius.

Keywords: ν-e; neutrino-electron scattering.

DOI: https://doi.org/10.31349/SuplRevMexFis.3.020711

1. Introduction

The standard model (SM), proposed by S. Glasgow, S. Weinberg, and A. Salam in the '60s, has proven to be an accurate theory. This theory has been verified in several physical observables by multiples experimental collaborations. Nowadays, we are in a period in which it is necessary to perform precision tests to confirm the SM predictions and therefore be able to search for new physics reliably. In the neutrino sector, we can use several scattering processes involving precision tests to make accurate measurements of SM parameters. One of these processes is the neutrino scattering with electrons [1, 2], due to its pure leptonic character, has been helpful to provide clear signatures in different predictions of the SM, such as the existence of Neutral Currents [3–6] in the Gargamelle experiment of CERN in 1973 [7]. Furthermore, due to its purely leptonic nature, it can provide us with several precision tests on electroweak (EW) parameters such as accurate measurements of the weak mixing angle. In addition, most of the Next Leading Order (NLO) radiative corrections of this scattering process can be evaluated analytically and therefore can serve as a prototype for more complex scattering cases such as the neutrino-nucleus scattering.

In addition, the neutrino-electron scattering radiative corrections have flavor-dependent contributions that are particular to neutrino interactions. Typically, this flavor-dependent correction is related to the neutrino charge radius and, by itself, is a new test of the SM [8–12].

Once Takaki Kajita and Arthur B. McDonald confirmed the neutrino oscillation mechanism, the experimental development in this sector has been stunning, and we expect high precision measurements in the near future. In particular, the search for the existence of a CP-violating phase has motivated the building of long-baseline experiments, where we expect intense neutrino beams. Measurements of the neutrino-electron scattering process with a high sensitivity to measure their radiative corrections will take place in their near detectors (ND).

In this work, we will explore the sensitivity to the radiative corrections of the neutrino-electron scattering that one of this future near detectors (such as DUNE-PRISM [13, 14]) will have and discuss the possibility of identifying the contribution of an effective neutrino charge radius [10, 12] that is gauge independent. A more detailed explanation of this work can be found in Ref. [15].

2. The neutrino-electron scattering

As already mentioned, neutrino-electron scattering is a process predicted by the SM. For the case of the electron neutrino, there is a charged component in this interaction. In this work, we will focus on the process of muon-(anti)neutrino scattering with electrons. This interaction only involves leptons and is a neutral current process mediated by the Z boson. This process can test the SM at low energies of the weak mixing angle, and with it, we can search for the possible existence of an effective neutrino charge radius (NCR).

At tree-level, an expression of the differential cross-section of the $\nu_\mu(\bar{\nu}_\mu)e^-$ scattering in terms of the electron recoil energy, T, is as follows

$$\frac{d\sigma}{dT}=\frac{2m_eG_F^2}{\pi}\left\{g_L^2+g_R^2\left(1-\frac{T}{E_\nu}\right)^2-g_Rg_Lm_e\frac{T}{E_\nu^2}\right\}, \quad (1)$$

where m_e is the electron mass, G_F is the Fermi constant, and E_ν is the energy of the incident neutrino. For this equation, the coupling constants g_L and g_R are defined as

$$g_L=\frac{1}{2}-\sin^2\theta_W, \quad (2a)$$

and

$$g_R = -\sin^2\theta_W\,, \tag{2b}$$

for the case of $\nu_\mu e^-$, with θ_W the weak mixing angle. While for $\bar{\nu}_\mu e^-$ we interchange the coupling constants, $g_L \leftrightarrow g_R$.

2.1. Radiative corrections

If we move to the NLO, the radiative corrections of the neutrino-electron scattering can be divided in two, depending on their dynamic origin. Refs. [16–24] present a more in-depth study on the corrections of this process. One of these is the quantum electrodynamic (QED) corrections, which involve creating and absorbing photons in the electronic current, *e.g.*, as illustrated in Fig. 1a). The other is the electroweak (EW) corrections due to the exchange of W and Z bosons, as we can see in Fig. 1b).

Considering the corrections mentioned above to this process, the expression of the differential cross-section for the $\nu_\mu e^-$ scattering is

$$\begin{aligned}\frac{d\sigma'}{dT} = \frac{2m_e G_F^2}{\pi}\Bigg(& g_L'^2(T)\left[1+\frac{\alpha}{\pi}f_-(z)\right] \\ &+ g_R'^2(T)\left[1-\frac{T}{E_\nu}\right]^2\left[1+\frac{\alpha}{\pi}f_+(z)\right] \\ &- g_R'(T)g_L'(T)m_e\frac{T}{E_\nu^2}\left[1+\frac{\alpha}{\pi}f_{+-}(z)\right]\Bigg),\end{aligned} \tag{3}$$

where α is the fine-structure constant, the contribution of the QED corrections is enclosed into the $f(z)$ functions, that depend on $z = T/E_\nu$. Refs. [15, 16] show the explicit forms of these functions. On the other hand, the EW corrections contribution is into the new coupling constants that depend on the electron recoil energy T:

$$g_L'(T) = \rho_{\rm NC}\left(\frac{1}{2} - \kappa_{\nu_l}(T)\sin^2\theta_W^{(m_Z)}\right) \tag{4a}$$

and

$$g_R'(T) = -\rho_{\rm NC}\kappa_{\nu_l}(T)\sin^2\theta_W^{(m_Z)}\,, \tag{4b}$$

where $\sin^2\theta_W^{(m_Z)}$ is $\sin^2\theta_W$ calculated at the m_Z scale. Note that the expression of the differential cross-section for the $\bar{\nu}_\mu e^-$ scattering is similar to Eq. (3), but the coupling constants must be swapped $g_L' \leftrightarrow g_R'$, while the functions $f(z)$ stay unswapped.

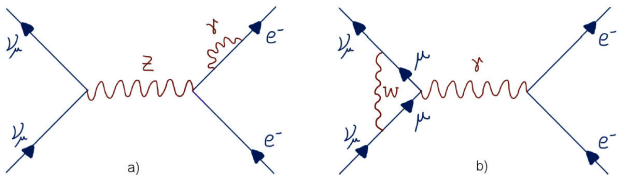

FIGURE 1. Illustrative Feynman diagrams for high order radiative corrections from a) QED, $e\gamma e$ vertexes and b) EW, $\mu W \nu_\mu$ vertices. Adapted from Ref. [15].

In this approximation, $\rho_{\rm NC}$ is independent of the electron recoil energy, T, and has a numerical value of $\rho_{\rm NC} = 1.014032$ (see Refs. [15,19] for its analytical expression). On the other hand, $\kappa^{(\nu_\mu,e)}(T)$ depends on T or, equivalently, to the square 4-momentum transfer $q^2 = -2m_eT$ and will be expressed as [19]:

$$\begin{aligned}\kappa_{\nu_l}(q^2) = 1 - \frac{\alpha}{2\pi\hat{s}^2}\Bigg(&\sum_i\left[C_{3i}Q_i - 4\hat{s}^2Q_i^2\right]J_i(q^2) - 2J_l(q^2) \\ &+ \ln c\left[\frac{1}{2} - 7\hat{c}^2\right] + \frac{\hat{c}^2}{3} + \frac{1}{2} + \frac{\hat{c}_\gamma}{\hat{c}^2}\Bigg),\end{aligned} \tag{5}$$

where s and c represent the sine and cosine of θ_W, respectively, and the hats over the parameters indicate their calculated values at the m_Z scale, $\hat{c}_\gamma = (19/8) - (17/4)\hat{s}^2 + 3\hat{s}^4$. The sum is over all the charged fermions, and an additional factor of three has to be considered for the quarks color degree of freedom, here Q_i represents the electric charge, C_{3i} is twice the third component of weak isospin and

$$J_i(q^2) = \int_0^1 dx x(1-x)\ln\left(\frac{m_i^2 - q^2x(1-x)}{m_Z^2}\right), \tag{6}$$

where m_i is the mass of the i fermion. The $2J_k(q^2)$ term of Eq. (5) plays an essential role since it contains the flavor dependence of the incident neutrino. For this work, we assume a ν_μ flux, thus we will have $2J_\mu(q^2)$.

In a first approximation, taking a monoenergetic neutrino beam, and considering the differential cross-sectional deviation at tree level defined as:

$$R_{\rm X} := \frac{\frac{d\sigma_{\rm X}'}{dT} - \frac{d\sigma}{dT}}{\frac{d\sigma}{dT}}\,, \tag{7}$$

where X represents the EW, QED, or the sum of both corrections, we observe an asymmetric relation between neutrino and antineutrino scattering in the case of EW radiative corrections [15], while for the QED corrections, the neutrino case is the same as for the antineutrino, as shown in Fig. 2. Considering both EW and QED radiative corrections, the antineutrino electron scattering process always has positive behavior, as opposed to the case of neutrinos, where the effect of both contributions causes a change of sign at a certain energy threshold.

2.2. Neutrino charge radius

We focus now on the $\kappa_{\nu_l}(q^2)$ of Eq. (5). This correction depends on the process under study, *e.g.*, on the neutrino flavor. Therefore, we can decompose this expression into two parts. On the one hand, the common expression for all neutrino flavors, $\kappa_\nu(q^2)$, is

$$\begin{aligned}\kappa_\nu(q^2) = 1 - \frac{\alpha}{2\pi\hat{s}^2}\Bigg(&\sum_i\left[C_{3i}Q_i - 4\hat{s}^2Q_i^2\right]J_i(q^2) \\ &+ \ln c\left[\frac{1}{2} - 7\hat{c}^2\right] + \frac{\hat{c}^2}{3} + \frac{\hat{c}_\gamma}{\hat{c}^2}\Bigg),\end{aligned} \tag{8}$$

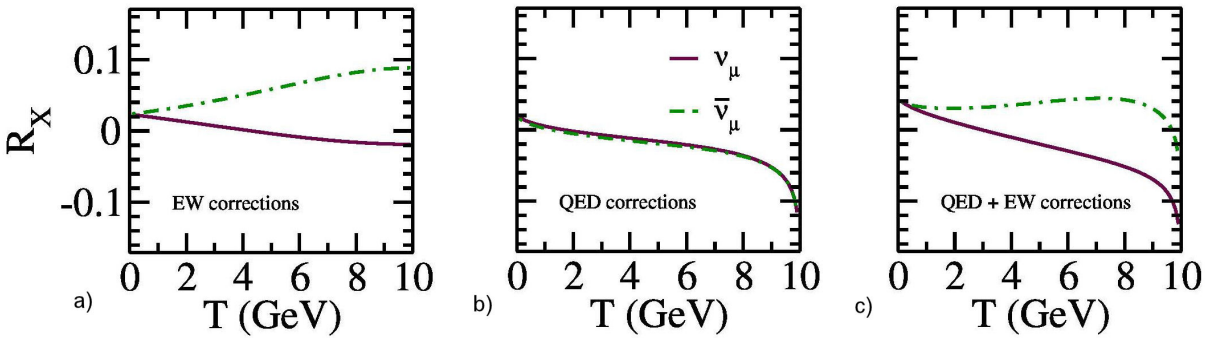

FIGURE 2. Radiative corrections ratio for neutrino and antineutrino beam modes for fixed neutrino energy of 10 GeV. a) EW corrections contribution, b) QED corrections contribution, and c) total contributions. Adapted from Ref. [15]

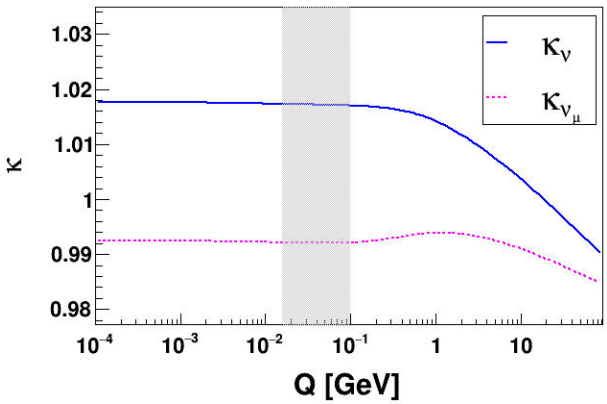

FIGURE 3. κ_ν and κ_{ν_μ} dependence on $Q \equiv -q^2$. The solid blue line corresponds to κ_ν, Eq. (8), while the dashed magenta line corresponds to κ_{ν_μ}, Eq. (5). The shaded area shows the electron recoil energy region where we study the radiative corrections effect and the experimental sensitivity to the NCR. Adapted from Ref. [15].

while the contribution that depends only on the neutrino flavor will be

$$-\frac{\alpha}{2\pi\hat{s}^2}\left(-2J_l(q^2)+\frac{1}{2}\right). \tag{9}$$

If we evaluate the content in parentheses in $q = 0$, we have

$$-2J_l(0)+\frac{1}{2}=\frac{1}{6}\left(3-2\ln\left[\frac{m_l^2}{m_Z^2}\right]\right), \tag{10}$$

and we obtain an expression associated with the neutrino charge radius (NCR):

$$\left\langle r^2_{\nu_l}\right\rangle = \frac{G_F}{4\sqrt{2}\pi^2}\left(3-2\ln\left[\frac{m_l^2}{m_W^2}\right]\right), \tag{11}$$

whose numerical value for the μ neutrino flavor is $\left\langle r^2_{\nu_\mu}\right\rangle = 2.4\times10^{-33}$ cm^2 [25].

The common contribution for all neutrino flavors, $\kappa_\nu(q^2)$, has a value of 1.0176 at $q^2 = 0$. On the other hand, if we include the term associated with the μ flavor NCR, we have $\kappa_{\nu_\mu}(q^2) = 0.9925$. We can see the behavior of these κs in Fig. 3. It is possible to see the contribution of the NCR, which is around 3 %.

3. The DUNE near detector case

One of the neutrino experiments with the most challenging neutrino physics program for the near future is the Deep Underground Neutrino Experiment (DUNE), whose main motivation is to search for the existence of a CP-violating phase. The baseline is related to the distance and the neutrino energy ratio (L/E) of the experimental setup. DUNE will consist of two neutrino detectors corresponding to a long and a short baseline. The far detector (FD), [26, 27] will be located at the Sanford Underground Research Laboratory with 40 kt at 1,300 km downstream of the source. One of the configuration options for the near detector (ND), is the PRISM detector [13, 14, 28], which will be set up at 574 m from the beam target located in Illinois at the Fermi National Accelerator Laboratory (Fermilab). PRISM would use the same Liquid Argon Time Projection Chambers (LAr TPC) technology as the DUNE FD and movable off-axis up to $3.6°$. This moving detector peculiarity allows different fluxes and spectra (as illustrated in Fig. 4). In this way, the systematic uncertainties of the flux and cross-section would be decreased, thus obtaining high sensitivity in the measurement of neutrino interactions.

We computed the expected number of events for neutrino scattering off electrons to explore the feasibility of using the DUNE-PRISM detector to study its radiative corrections. For this, we consider the expected fluxes in PRISM at different angular locations reported in Ref. [29] and shown in Fig. 4.

For the number of targets, we consider the electrons contained in the mass of 75 t of Liquid Argon that PRISM expects to have [14]; the number of protons on target per year equal to 1.1×10^{21} POT/year [29]; and an estimation to run for 7 years, dividing half of the period in neutrino mode and the other half in antineutrino mode.

With these considerations, in the next section, we will discuss the results of having calculated the expected number of events of the neutrino-electron scattering process at tree level and considering the radiative corrections, with and without the NCR contribution.

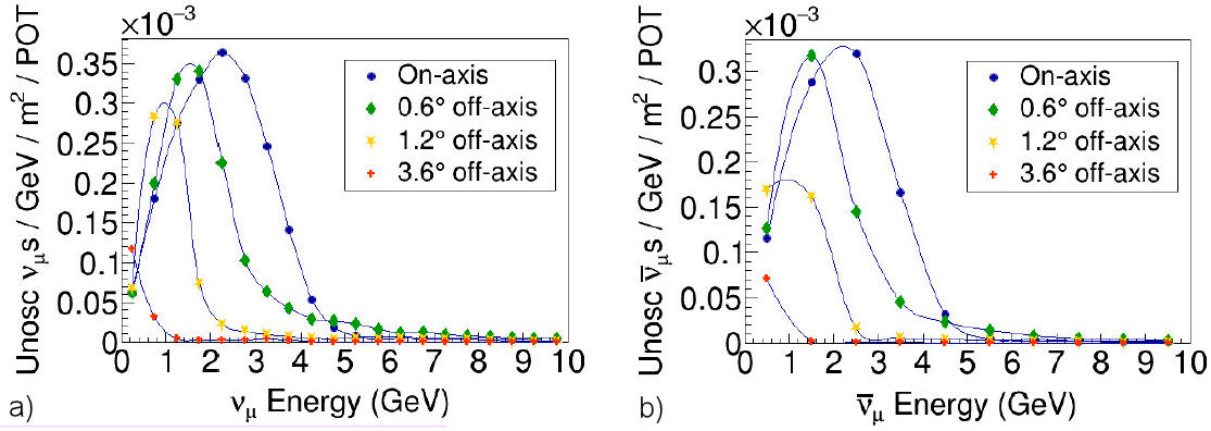

FIGURE 4. Fluxes at several off-axis locations [29]. Left panel: Neutrino mode. Right panel: antineutrino mode. The different symbols stand for the simulated data, while the lines show the corresponding interpolation. Adapted from Ref. [15].

4. Results and discussion

Radiative corrections always increase the expected number of events for the antineutrino channel; this is opposite to the neutrino case, where we expect a decrease in the number of events, starting around 0.7 GeV. For this reason, we consider two different electron recoil energy thresholds: One with a 0.2 GeV energy threshold and the other with 0.7 GeV. These selections will maximize the differences between the number of events expected at the tree level and the one with radiative corrections for the neutrino case.

In the antineutrino case, for an energy range from 0.2 GeV to 10 GeV and an on-axis flux, the expected number of events with radiative corrections is higher than the expected at tree level, as shown in Table 1. When including the NCR contribution into the corrections, the number of events is still higher than at the tree level but is lower than expected without this contribution. We illustrate this behavior in Fig. 5b), where for the first bin is clear that the differences between the number of events with corrections and at tree level are bigger than the statistical error.

On the other hand, in the neutrino case, for an energy range from 0.2 GeV to 10 GeV, and for an on-axis flux, we observe in Table I that the number of events with radiative corrections is lower than expected at tree level. While including the NCR contribution to the corrections, the number of events is still lower than the tree level but higher than expected without this contribution. We show this behavior in Fig. 5a). Now, as mentioned before, for the $\nu_\mu e^-$ taking an energy range from 0.7 GeV to 10 GeV maximizes the difference between the number of events expected with radiative corrections and at tree level, we see this effect in the last row of Table I.

A more detailed study [15] observed that the difference between the number of events with radiative and tree-level corrections is larger than the statistical error up to an off-axis flux of (anti)neutrinos at $1.8°$. In this work, we present only the on-axis case, but the results to the off-axis positions can be found at [15].

To conclude this study, we performed a χ^2 analysis to estimate the sensitivity to radiative corrections that we would have in an experiment such as PRISM. To do so, we defined the function

TABLE I. The first two rows are the number of events for $\bar{\nu}_\mu$ and ν_μ scattering with electrons respectively for an energy range of 0.2 to 10 GeV, while the third and last row is the number of events for $\nu_\mu e$ scattering for an energy range of 0.7 to 10 GeV. In all cases, the number of events at the tree level is considered and with and without the NCR. Here σ_{stat} is the statistical error and Δ is the difference between the number of events at tree level and radiative corrections (with and without NCR).

	Number of Events					
			Without NCR		With NCR	
	Tree-level	σ_{stat}	EW+QED	Δ	EW+QED	Δ
$\bar{\nu}_\mu$	18775	137	19931	1156	19447	672
ν_μ	27134	165	25859	-1275	26567	-567
ν_μ	19947	141	18715	-1232	19318	-629

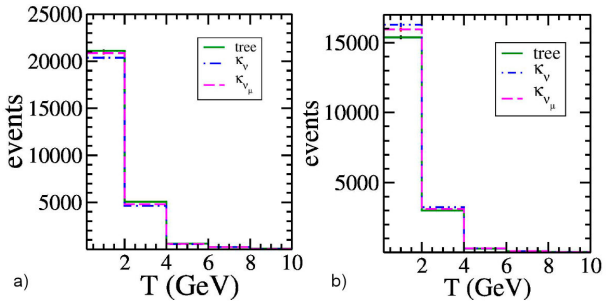

FIGURE 5. Comparison among the number of ν_μ a) and $\bar{\nu}_\mu$ b) event expectations at tree-level (solid black line) and considering radiative corrections, with and without neutrino charge radius (dashed magenta and dot-dashed blue line, respectively). Adapted from Ref. [15].

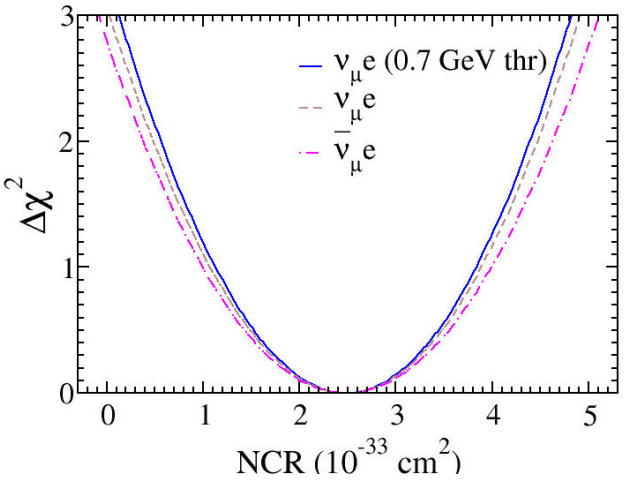

FIGURE 6. Expected sensitivity to NCR, for a 3 % systematic error, to the electroweak radiative corrections. Brown dashed and magenta dot-dashed lines show the case of a 0.2 GeV threshold for the ν and $\bar{\nu}$ scattering. The blue line considers a 0.7 GeV ν scattering threshold. Adapted from Ref. [15].

$$\chi^2 = \sum_{i=1}^{5} \frac{(N_i^{\rm exp} - N_i^{\rm theo})^2}{(\sigma_{\rm stat}^2 + \sigma_{\rm syst}^2)_i}\,, \tag{12}$$

and $\Delta\chi^2 = \chi^2 - \chi^2_{\rm min}$, where $\chi^2_{\rm min}$ is the minimum value of χ^2, i stands for the energy bin, $N^{\rm exp}$ defines the number of events predicted by the SM, considering the radiative corrections, and $N^{\rm theo}$ denotes the theoreticall number of events calculated for different values of κ (Eq. 5). $\sigma_{\rm stat} = \sqrt{N^{\rm exp}}_i$ are the statistical uncertainties and $\sigma_{{\rm syst}\,i}$ represent the systematic uncertainties.

If we take a systematic error of 3%, we observe that at 1σ precision, an experiment like PRISM could be sensitive to distinguish the NCR for the antineutrino channel in a range from 1.0 to 4.0×10^{-33} cm^2. In constrast, the neutrino channel is sensitive in a range from 1.1 to 3.9×10^{-33} cm^2 considering an energy threshold of 0.2 GeV, while for an energy threshold of 0.7 GeV is sensitive in a range from 1.1 to 3.8×10^{-33} cm^2. Thus, with these assumptions, it can achieve a higher than 90% confidence level of NCR sensitivity, as shown in Fig. 6.

Interestingly, the current constraint reported in the PDG for the $\nu_\mu e^-$ is in the range of -5.3 to 6.8×10^{-33} cm^2 [22], which is still consistent with the absence of NCR.

5. Conclusions

We have studied the sensitivity of the DUNE-PRISM-like detector as an example of future near detectors, to the radiative corrections in the neutrino-electron scattering process. Due to its higher statistics, the neutrino beam mode will better determine the radiative corrections and possibly the NCR if the systematic uncertainties are under control. While for the antineutrino beam mode, despite the lower statistics, compared to the neutrino mode, our analysis shows a reasonable possibility of measuring the radiative corrections and even the NCR with the lower energy bin. We illustrated that a systematic error of the order of 3 % gives reasonable expectations to measure the NCR with an error of the order of 1.5×10^{-33} cm^2.

Acknowledgments

This work was supported by CONACYT-Mexico grant A1-S-23238, SNI (Sistema Nacional de Investigadores). CAM acknowledges FAPESP Grant process no. 2014/19164-6.

1. P. Vilain *et al.* [CHARM-II], Precision measurement of electroweak parameters from the scattering of muon-neutrinos on electrons, *Phys. Lett. B* **335** (1994) 246, https://doi.org/10.1016/0370-2693(94)91421-4.

2. C. Anderson *et al.* [ArgoNeuT], First Measurements of Inclusive Muon Neutrino Charged Current Differential Cross Sections on Argon, *Phys. Rev. Lett.* **108** (2012) 161802, https://doi.org/10.1103/PhysRevLett.108.161802.

3. S. L. Glashow, Partial Symmetries of Weak Interactions, *Nucl. Phys.* **22** (1961) 579 , https://doi.org/10.1016/0029-5582(61)90469-2.

4. S. Weinberg, A Model of Leptons, *Phys. Rev. Lett.* **19** (1967) 1264, https://doi.org/10.1103/PhysRevLett.19.1264.

5. S. L. Glashow and S. Weinberg, Natural Conservation Laws for Neutral Currents, *Phys. Rev. D* **15** (1977) 1958, https://doi.org/10.1103/PhysRevD.15.1958.

6. A. Salam, Weak and Electromagnetic Interactions, *Conf. Proc. C* **680519** (1968) 367 https://doi.org/10.1142/9789812795915_0034.

7. F. J. Hasert *et al.* [Gargamelle Neutrino], Observation of Neutrino Like Interactions Without Muon Or Electron in the Gargamelle Neutrino Experiment, *Phys. Lett. B* **46** (1973) 138, https://doi.org/10.1016/0370-2693(73)90499-1.

8. S. Sarantakos, A. Sirlin and W. J. Marciano, Radiative Corrections to Neutrino-Lepton Scattering in the SU(2)-L x U(1) Theory, *Nucl. Phys. B* **217** (1983) 84, https://doi.org/10.1016/0550-3213(83)90079-2.

9. J. L. Lucio, A. Rosado and A. Zepeda, Neutrino Charge in the Linear R(xi) Gauge, *Phys. Rev. D* **29** (1984) 1539 https://doi.org/10.1103/PhysRevD.29.1539.

10. L. G. Cabral-Rosetti, J. Bernabeu, J. Vidal and A. Zepeda, Charge and magnetic moment of the neutrino in the background field method and in the linear R-L(xi) gauge, *Eur. Phys. J. C* **12** (2000) 633 , https://doi.org/10.1007/s100520000304.

11. K. Fujikawa and R. Shrock, On a neutrino electroweak radius, *Phys. Rev. D* **69** (2004) 013007, https://doi.org/10.1103/PhysRevD.69.013007.

12. J. Papavassiliou, J. Bernabeu, D. Binosi and J. Vidal, The Effective neutrino charge radius, *Eur. Phys. J. C* **33** (2004) S865, https://doi.org/10.1140/epjcd/s2003-03-920-7.

13. D. Hongyue [DUNE], DUNE Near Detector with focus on cross section and prospects from the oscillation perspective, *PoS* **NuFact2017** (2018) 058, https://doi.org/10.22323/1.295.0058.

14. V. De Romeri, K. J. Kelly and P. A. N. Machado, DUNE-PRISM Sensitivity to Light Dark Matter, *Phys. Rev. D* **100** (2019) 095010, https://doi.org/10.1103/PhysRevD.100.095010.

15. O. G. Miranda, G. Moreno-Granados and C. A. Moura, Sensitivity of accelerator-based neutrino experiments to neutrino-electron scattering radiative corrections, *Phys. Rev. D* **104** (2021) 013007, https://doi.org/10.1103/PhysRevD.104.013007.

16. J. N. Bahcall, M. Kamionkowski and A. Sirlin, Solar neutrinos: Radiative corrections in neutrino - electron scattering experiments, *Phys. Rev. D* **51** (1995) 6146, https://doi.org/10.1103/PhysRevD.51.6146.

17. M. Passera, QED corrections to neutrino electron scattering, *Phys. Rev. D* **64** (2001) 113002, https://doi.org/10.1103/PhysRevD.64.113002.

18. M. Passera, QED corrections to the scattering of solar neutrinos and electrons, *J. Phys. G* **29** (2003) 141 https://doi.org/10.1088/0954-3899/29/1/315.

19. A. Sirlin and A. Ferroglia, Radiative Corrections in Precision Electroweak Physics: a Historical Perspective, *Rev. Mod. Phys.* **85** (2013) 263 https://doi.org/10.1103/RevModPhys.85.263.

20. A. Ferroglia, G. Ossola and A. Sirlin, The Electroweak form-factor kappa-hat (q**2) and the running of sin**2 theta-hat (W), *Eur. Phys. J. C* **34** (2004) 165 https://doi.org/10.1140/epjc/s2004-01604-1.

21. J. Erler and R. Ferro-Hernández, Weak Mixing Angle in the Thomson Limit, *JHEP* **03** (2018) 196 https://doi.org/10.1007/JHEP03(2018)196.

22. P.A. Zyla *et al.* [Particle Data Group], Review of Particle Physics, *PTEP* **2020** (2020) 083C01 https://doi.org/10.1093/ptep/ptaa104.

23. O. Tomalak and R. J. Hill, Theory of elastic neutrino-electron scattering, *Phys. Rev. D* **101** (2020) 033006 https://doi.org/10.1103/PhysRevD.101.033006.

24. I. Bischer and W. Rodejohann, General Neutrino Interactions at the DUNE Near Detector, *Phys. Rev. D* **99** (2019) 036006 https://doi.org/10.1103/PhysRevD.99.036006.

25. C. Giunti and A. Studenikin, Neutrino electromagnetic interactions: a window to new physics, *Rev. Mod. Phys.* **87** (2015) 531 https://doi.org/10.1103/RevModPhys.87.531.

26. B. Abi *et al.* [DUNE], Volume I. Introduction to DUNE, *JINST* **15**, no.08, (2020) T08008 https://doi.org/10.1088/1748-0221/15/08/T08008.

27. B. Abi *et al.* [DUNE], Deep Underground Neutrino Experiment (DUNE), Far Detector Technical Design Report, Volume II DUNE Physics, [arXiv:2002.03005 [hep-ex]].

28. C. Vilela, (2018), presented at Physics Opportunities in the Near DUNE Detector hall (PONDD 2018), Fermilab, IL, USA: https://doi.org/10.5281/zenodo.2642370

29. L. Fields, DUNE Fluxes, https://home.fnal.gov/~ljf26/DUNEFluxes/

30. A. Abed Abud *et al.* [DUNE], Deep Underground Neutrino Experiment (DUNE) Near Detector Conceptual Design Report, [arXiv:2103.13910 [physics.ins-det]].